Journal of Thermal Analysis, Vol. 51 (1998) 161-171

THERMAL ANALYSIS OF AQUEOUS MICELLAR SOLUTIONS
Study of some structural transitions and of solute-surfactant complexes

K. Ballerat-Busserolles, S. Rassinoux, G. Roux-Desgranges and A. H. Roux

Lab. Thermodynamique et Génie Chimique, UPRES A CNRS 6003, Université Blaise Pascal, 63177 Aubière Cedex, France

Abstract

A micro differential temperature scanning calorimeter was used to characterize the structural changes between different types of micelles in aqueous solutions of ionic surfactants: anionic – sodium dodecylsulfate (SDS) – and cationic – hexadecyltrimethyl ammonium bromide (CTAB). Moreover, this technique allowed to confirm the existence of peculiar types of complexes between surfactants and selected solutes. In SDS solutions containing polyethylene glycols (PEG), the presence of complexes formed by small micelles adsorbed along the chains of the polymers was evidenced in the case of long enough polymer chains. In CTAB-phenol solutions, due to strong interactions between the polar heads of surfactant and phenol, molecular complexes of a composition of 1:1 molar ratio have been characterized. Depending on the ratio [phenol]/[CTAB], the rheological behaviour was found to change from fluid to viscoelastic and gel-like solutions, owing to the growth of elongated rod-like micelles. With entangled worm-like micelles, the important role of kinetics to reach the thermodynamic equilibria was shown.

Keywords: differential scanning calorimetry, phenol, polyethylene glycols, surfactants

Introduction

Thermal analysis techniques are useful tools to evidence structural transitions occurring between two physical states of the matter as well as in a given phase. More particularly, temperature scanning differential microcalorimeters allow to detect even weak interactions in solutions through analysis of DSC curves. However, this sensitive technique has only found limited applications in studying aqueous micellar systems [1–5]. In these solutions several structural changes are observed with the increase in surfactant concentration and temperature. Moreover, the addition of a third component, depending on its chemical nature or structure, induces important structural modifications of the medium as a result of privileged interactions between surfactant and solute.

0368–4466/98/ $ 5.00

Akadémiai Kiadó, Budapest
Kluwer Academic Publishers, Dordrecht

To illustrate the application of thermal analysis to micellar solutions containing an interacting solute, two quite different characteristic systems were selected. The first type of systems contained water-soluble polymers in solution with anionic surfactants. In these systems complexes are typically formed, in which the surfactant is aggregated as small micelles adsorbed onto the polymer chains [6–12]. The chain length of the polymer is of some importance since this complex is occurring only when the polymer is sufficiently long to wrap around a micelle [10]. Water-sodium dodecylsulfate (SDS)-polyethylene glycols (PEG), which have been extremely widely investigated, were chosen as model systems.

The second type of systems investigated included aqueous solutions of cationic surfactants in the presence of selected aromatic molecules. In this case very strong complexes may be formed when the solutes are capable of establishing specific interactions with the polar heads of surfactants, leading generally to spectacular changes in the rheology of the solutions [4, 13–16]. Depending on the concentrations of surfactant and solute as well as on the temperature, viscoelastic, even gel-like, solutions are often observed. The properties of such thermoreversible gels can be investigated by DSC analysis to determine the molar composition of the complex obtained in the case of the system water-hexadecyltrimethylammonium bromide (CTAB)-phenol.

Experimental

Sodium dodecylsulphate (SDS) with a purity better than 99% was purchased from Merck and hexadecyltrimethylammonium bromide (CTAB) was a puriss. grade from Fluka. They were used without further purification after being dried several days under vacuum at a temperature below 50°C. Phenol (purity 99%) and polyethylene glycols were supplied by Aldrich. The polydispersity of the polymers, as specified by Aldrich, was 1.1 and 1.5 for PEG 400 and 10000, respectively (this number is representative of the mean molar mass of the PEG).

The experiments were carried out using a micro differential scanning calorimeter (micro DSC I, Setaram, France). This apparatus, based on the Calvet principle, has been described previously [17]. The micro DSC is able to work according to several procedures. In the present case the continuous scanning mode was appropriate to evidence structural transitions in solution. It allows to measure the differential thermal flux between the cells and the thermostatted metallic block the temperature of which is scanned at a constant rate in a selected range monitored by a computer. The thermal flux is then converted into volumetric heat capacities of the fluid by means of calibration curves previously established by taking into account the sensitivity of the thermopiles, the true rate of temperature scanning and the real temperature. Additionally, the calibration is controlled using vacuum and water. The heat capacity and density of water as a function of

temperature being well-known [18, 19], the heat capacities for the unknown liquid filling the cell can be determined with an estimated uncertainty of 10^{-3} J K^{-1} cm^{-3} between 2 and 80°C.

In order to control the thermal history of samples and to obtain reproducible DSC curves with each micellar solution a strict experimental protocol was respected. Solutions were introduced into the measurement cell at the maximum temperature and left until thermal equilibrium was established. Then the consecutive scans at the fixed rate along the investigated range of temperature were started beginning by a cooling followed by a heating and finally again a cooling. Between each sequence, a delay time at the limit temperatures was imposed to let thermal equilibrium settle. Only the two last scans in heating and cooling mode were recorded to obtain reproducible data concerning the peaks of fusion and crystallization. The selected range of temperature was –7 to 70°C at a scanning rate of 0.04 K min^{-1} and from 1 to 70°C at 0.2 K min^{-1}. The scanning rates were chosen sufficiently low to stay all the time close to the thermodynamic equilibrium.

Results and discussion

Binary solutions Water+surfactant

DSC curves were recorded with solutions of SDS and CTAB over a wide range of surfactant concentrations between 0.05 and 0.4 mol kg^{-1} for SDS and 0.01 to 0.2 mol kg^{-1} for CTAB. Their respective profiles are very similar in the heating mode as well as in the cooling mode for different SDS and CTAB concentrations. DSC curves, obtained at a scanning rate of 0.04 K min^{-1} for the selected concentration 0.15 mol kg^{-1} with both surfactants, are depicted in Fig. 1.

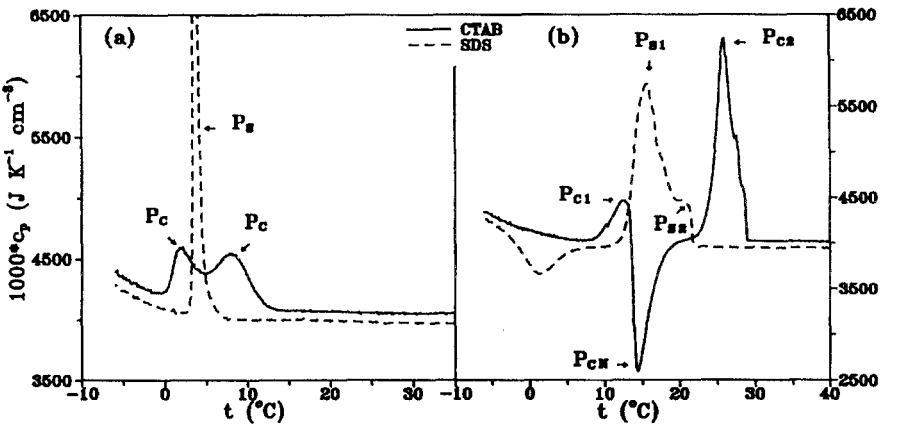

Fig. 1 DSC curves recorded in cooling (a) and heating (b) modes on SDS and CTAB aqueous solutions at the concentration of 0.15 mol kg^{-1} with a scanning rate of 0.04 K min^{-1}

The observed peaks illustrate the behaviour of surfactant solutions close to the Krafft point, where the surfactant precipitates when its concentration exceeds the solubility. However, depending on the sign of the thermal gradient, the observed temperatures of the peaks differ by about 10 K between heating and cooling, as for the freezing of water super cooling occurs. In the cooling mode a single and sharp peak appears for SDS, whereas for CTAB two distinct steps are marked by two broad peaks, the amplitudes of which depend on the CTAB concentration. In the heating mode several peaks of fusion can be observed with magnitudes increasing and positions shifted regularly towards higher temperatures as the surfactant concentration increases. In the case of SDS solutions, an exothermic peak is followed by two overlapping endothermic peaks (labelled P_{s1} and P_{s2}) corresponding to the melting of SDS crystals containing different amounts of water. For CTAB, the peak (P_{c1}) at the lowest temperature is endothermic, and it is followed by an exothermic peak (P_{cN}) and two overlapping endothermic peaks P_{c2}. Due to supercooling, the DSC curves in the cooling mode were less reproducible and consequently only the heating curves are discussed further.

Characteristic temperatures of the DSC curves carry information on the structure of the micellar solutions. We have plotted in Fig. 2, as a function of the molality of surfactant, the temperatures corresponding to the end of fusion since they can be unambiguously observed in the different curves recorded in the presence of the two surfactants. These temperatures are increasing almost linearly with the surfactant concentration but a change in the slope seems to occur around 0.15 mol kg^{-1} with SDS and around 0.08 mol kg^{-1} with CTAB. These break points are certainly in relation with the post micellar transitions taking place in

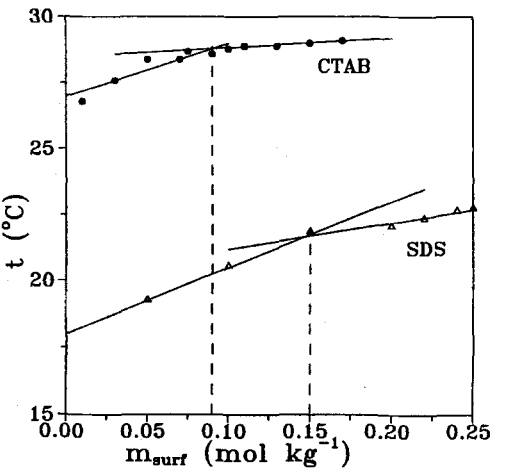

Fig. 2 Dependence of the temperature of the end of fusion *vs.* the surfactant concentration for SDS and CTAB

surfactant solutions such as those observed, for example for thermodynamic properties at 25°C, at 0.2 mol kg^{-1} with SDS [20] and 0.15 mol kg^{-1} in the case of CTAB [21, 22]. These postmicellar transitions have been attributed to changes in shape and size of micelles from spherical to cylindrical, accompanied by an enhance of counterion binding [21].

Ternary systems Water+SDS+PEG

The formation of well defined complexes between SDS and PEG owing to mainly hydrophobic interactions, when the polymer chain is sufficiently long, have been evidenced by several techniques [7–12, 23]. Our aim was to check the existence and stability of the complexes and, for this purpose, two quite different PEG's were compared in order to look at the role of the chain length: PEG 400, a small oligomer, and PEG 10000, a true polymer. For this comparison the amount of solute was kept constant at 2 wt.% while the concentration of surfactant was varied.

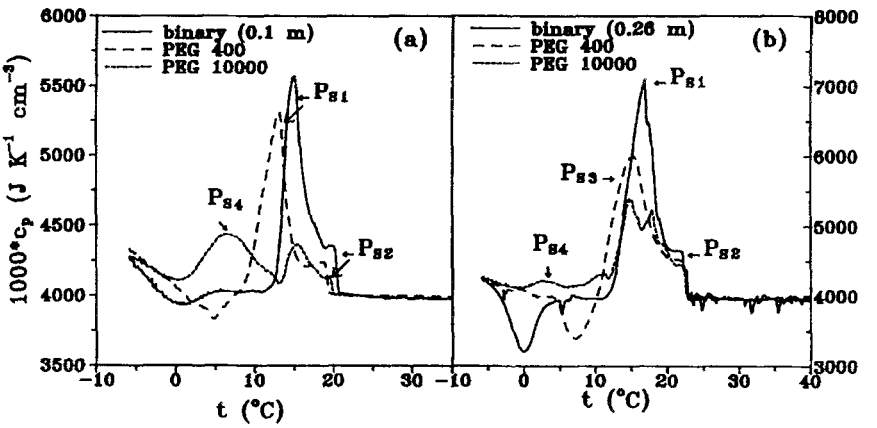

Fig. 3 DSC curves obtained in the heating mode with a scanning rate of 0.04 K min^{-1} on ternary systems water+SDS+2 wt.% PEG (400 and 10000) at two concentrations of SDS (a) 0.1 mol kg^{-1} and (b) 0.26 mol kg^{-1}

Typical DSC curves for two ternary systems where the SDS concentration is varied from below 0.2 mol kg^{-1} (the postmicellar concentration transition) to higher values, are presented in Fig. 3. For comparison, the DSC curves of the corresponding binary mixtures are also given. In the presence of PEG 400, two peaks (P_{s1} and P_{s2}) appear which are similar to those observed with binary systems, but they are slightly shifted towards lower temperatures. PEG 400 behaves like a small organic molecule depressing the Krafft temperature of the surfactant [24]. With the increase of SDS concentration, small peaks appear at temperatures lower than the main peak, then they overlap together with P_{s1} in broader endo-

thermic peak (P_{s3}). Such effects might be due to some mixed entities SDS-PEG 400 which are probably existing in more concentrated solutions.

The DSC curves obtained in the presence of PEG 10000 show particular features corresponding to structural changes in the solution. While the SDS concentration remains small the two characteristic peaks of the binary system are still present but their magnitudes are greatly reduced. In addition, a new broad peak (P_{s4}) appears at lower temperature which is gradually enlarged as the SDS concentration increases to 0.2 mol kg^{-1}. In contrast, beyond 0.2 mol kg^{-1} this peak progressively vanishes while a group of several overlapping peaks are replacing the typical peaks of the binary system. The evolution of the profiles of the curves along with the SDS concentration confirms the existence of a complex between SDS and PEG 10000. It is generally assumed that in the presence of sufficiently long water-soluble polymers (of molar masses up to about 4000 for PEG) monomers of SDS aggregate into micelles small than those in water [7, 8]. These small micelles are adsorbed onto the polymer chains until the 'saturation' of the polymer is attained. When SDS is in excess, free micelles having then a normal size are coexisting in solution with micelles bound to polymer. The stoichiometry of the complexes formed in the present system has been previously estimated, it yields a ratio between ethoxy groups (EO) of PEG and surfactant molecules [EO]/[SDS] close to 3 depending on the techniques of investigation [9–12, 25, 26]. As a consequence, for an amount of 2 wt.% of PEG 10000, the saturation of the polymer would be attained when the concentration of SDS is close to 0.2 mol kg^{-1}. Therefore, until this concentration is reached the presence of the broad peak P_{s4} with increasing intensity characterizes the progressive adsorption of micelles to form the complex. Obviously the peaks P_{s1} and P_{s2} characterizing normal free micelles are quite small since almost all SDS micelles are adsorbed on polymer chains. Beyond 0.2 mol kg^{-1}, free micelles are existing again in solution and the peaks corresponding to those of the binary system are now increasing with SDS concentration. However, the DSC curves appear more complicated in this range of concentration. Actually, normal free micelles, micelles bound onto polymer and presumably also micelles of different shapes due to the possible structural changes are present together in solution.

Ternary systems Water+CTAB+phenol

These micellar systems present some very interesting features concerning the drastic changes in structure when the temperature or the concentrations of solutes are slightly varied. With appropriate concentrations of phenol, the viscosity is sharply increasing to give gels for CTAB concentrations near 0.2 mol kg^{-1} [27]. Using DSC analysis, the existence of stable molecular complexes between CTAB and phenol responsible for the abnormal viscosity is confirmed when the variation of the ratio R=[phenol]/[CTAB] is examined.

In a first series of experiments, DSC curves are obtained at a scanning rate of 0.2 K min^{-1}, for solutions at a given CTAB concentration (0.1 mol kg^{-1}) and vari-

ous phenol concentrations. Some of the curves obtained in the heating mode are shown in Fig. 4. The recorded enthalpic peaks appear quite regular with a well-defined baseline, yielding characteristic temperatures (T) of the peaks and corresponding heats of fusion (ΔH relative to volume unit). The variation of these two

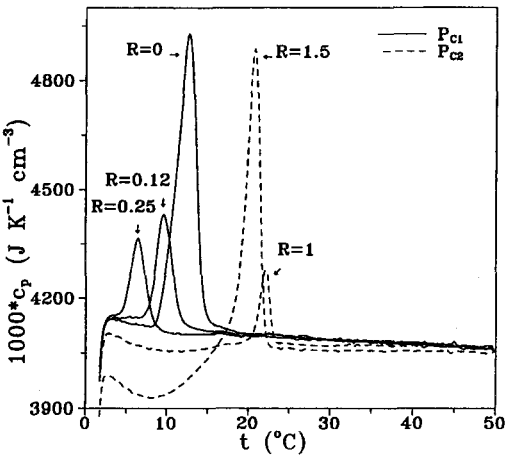

Fig. 4 DSC curves recorded with a heating rate of 0.2 K min^{-1} of the ternary system water+CTAB (0.1 mol kg^{-1})+phenol for different ratios R ([phenol]/[CTAB])

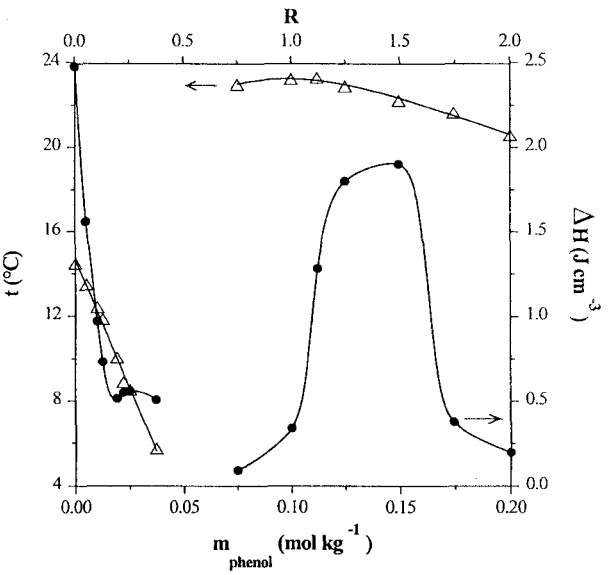

Fig. 5 Dependence of the temperatures of the peaks (Δ) and of the corresponding integrated heats of fusion (•) with the ratio R, obtained with a heating rate of 0.2 K min^{-1} for a CTAB concentration of 0.1 mol kg^{-1}

values are reported *vs.* the ratio R[phenol]/[CTAB] in Fig. 5. Along the phenol ratio, two domains can be defined in which the variations are different. In the first domain, up to R<0.5, like with the binary system (W+CTAB) a single peak (P_{c1}) is obtained. Its temperature (T_1=14.5°C for the binary system) is shifted towards lower temperatures almost linearly with R. The resulting heat of fusion (ΔH_1=2.5 J cm^{-3} for the binary system) is also sharply decreasing with R. When R is close to 0.5, in the temperature range studied, crystallization does not occur during the cooling scan and no peak of fusion is observed. In this domain (R<0.5) the peak P_{c1} corresponds to the fusion of CTAB crystals formed during the cooling cycle when the temperature is lower than the Krafft point. With the addition of phenol, the temperature of fusion decreases similarly as the Krafft point is lowered in the presence of classical hydrophobic solutes in ionic surfactant solutions [24]. The second domain, corresponding to R>0.5, is characterized by the presence of a different peak P_{c2} for which T and ΔH values also depend on R. The associated temperature T_2 remains constant close to 23°C up to R≈1 and then slightly decreases. The variation of ΔH_2 is more complicated and, over a narrow R range, is going through a maximum around R=1.5, and then vanishes for R>2. The variation of ΔH_2 reflects the stability of the phenol-CTAB complex which appears to be maximum for R between 1 and 1.5. When R is larger than 2, due to the excess of phenol, the complex does not exist any longer and thus the peak P_{c2} disappears.

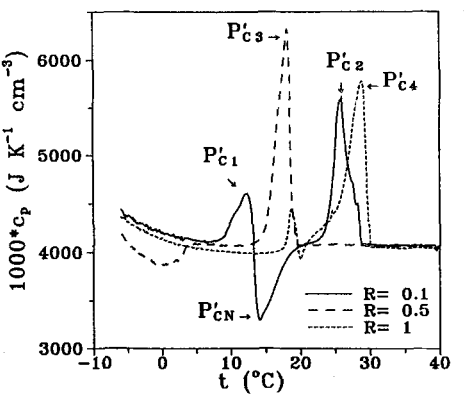

Fig. 6 DSC curves recorded with a heating rate of 0.04 K min^{-1} on the ternary system water+CTAB (0.1 mol kg^{-1})+phenol for different ratios R

In order to define more accurately the thermal behaviour of this complex, similar experiments were carried out at a scanning rate of 0.04 K min^{-1} between –6 and 70°C for different CTAB and phenol concentrations to cover a wider range of R. The DSC curves behave differently and are more complicated when compared to those recorded at a higher scanning rate. Some representative DSC curves are shown in Fig. 6 to illustrate the additional peaks appearing at a low

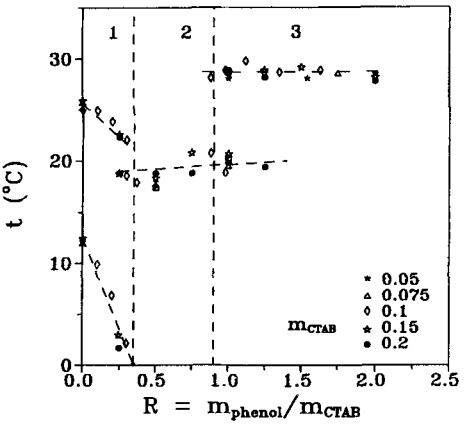

Fig. 7 Variation of the temperatures of the peaks recorded at a heating rate of 0.04 K min^{-1}, as a function of R for different CTAB concentrations

heating rate. When considering the same ratio R, independently of the CTAB concentration, similar DSC curves are recorded. The temperatures of the different peaks are plotted in Fig. 7 as a function of R. The similar dependence of T on R for a wide range of phenol and surfactant concentrations clearly evidences the existence of phenol-CTAB complexes. Three domains can be distinguished from close values of the characteristic temperatures of the peaks. As seen in Fig. 7, from R=0 to 0.4 (domain 1), the two peaks (P'_{c1}, P'_{c2}) separated by P'_{cN} are comparable to those present in the binary system shown in Fig. 1. They are progressively vanishing with the increase in phenol concentration (or with R). For $0.4<R<1$ (domain 2), P'_{c1} and P'_{c2} are not existing any longer, but a new peak P'_{c3} appears at a constant temperature T'_3 close to 19°C. Its area is maximum for R close to 0.5, then it vanishes. Further, when $R>0.8$ (domain 3) this peak is progressively replaced by another peak P'_{c4} at a constant higher temperature close to 28°C. Generally, at this low heating rate, the different peaks are overlapping and the difficulty of estimating the baselines does not allow determination of the respective associated heats of fusion with satisfactory accuracy.

The study conducted at two different scanning rates revealed the important role of the kinetics of the crystallization and fusion of the complexes to reach a thermodynamic equilibrium. At the higher rate the different mixed crystals are not fully separated and they melt together at the mean temperature of 23°C whereas at the lower rate two types of mixed crystals melting respectively at 19 and 28°C are identified.

The different domains of composition identified by DSC analysis can be correlated to the viscosity of the solutions at room temperature [27]. In domain 1, where the addition of phenol leads only to the depression of the Krafft point, solutions are fluid, becoming more and more viscous at the approach of the bound-

ary ($R \approx 0.4$). In domain 2, the viscoelastic trend is increasing up to gel formation when $R \rightarrow 1$. The existence of strong interactions between phenol molecules and the positive head groups of the surfactant at the interface of micelles, favours the stabilization of micelles. It leads to an important growth of elongated micelles reaching a maximum near $R = 1$ when one phenol molecule strongly interacts with one CTAB cation. With the increase of CTAB and phenol concentrations the entanglement of such worm-like micelles provides viscoelasticity, then gel-like tendencies are manifested [15]. In domain 3, at higher phenol ratio, the gel-like solutions are becoming less and less viscous since the excess of phenol prevents the formation of stable wormlike micelles. Such fragile structures are broken by thermal motion, the gelled solutions are suddenly becoming fluid over a narrow temperature range between 40 and 50°C, thus reflecting a change in structure of the gigantic micellar aggregates leading to much smaller entities [28]. This transition is thermoreversible in contrast to what is observed with polymer solutions for which the temperature does not affect rheological properties appreciably.

In spite of the sensitivity of DSC analysis to structural changes, the sudden variation of viscosity occurring with the increase in temperature is not revealed. No variations of enthalpy or heat capacity correlated to the observed rheological properties of the solutions with temperature were noticed in our experiments. However, recent parallel DSC analysis on the parent system water-CTAB-*o*-iodophenol [5] has permitted to evidence a variation of enthalpy associated with the thermal transition from viscoelastic to fluid solutions around 55°C, depending strongly on the heating rate and the time to restore viscoelasticity. This would suggest that in our present measurements, with phenol, either the process of gel formation is almost athermal or most likely the rate of this reaction is particularly low compared to the scanning rate.

Conclusion

DSC techniques proved to be an alternative tool to detect the change of physical state for polymer materials. However, such approach is not currently applied to the investigation of structural changes occurring in aqueous micellar solutions. The efficiency of micro DSC techniques has been demonstrated with SDS and CTAB aqueous solutions where the change of the micelle shape with surfactant concentration is clearly observed. Then, with ternary systems, the existence of complexes between surfactant and solute is asserted for weak complexes where micelles are adsorbed on long water-soluble polymers, as well as for strong complexes of a defined stoichiometry 1:1 existing in CTAB solutions, owing to electrostatic interactions involving the solute at the micellar interface. Additionally, DSC provides direct information on the energetics of structural transformations via enthalpy and heat capacity determinations.

References

1 H. Hirata, Y. Kanda and S. Ohashi, Colloid Polym. Sci., 270 (1992) 781.
2 S. Kaneshina and M. Yamanaka, J. Colloid Interface Sci., 140 (1990) 474.
3 M. J. Blandamer, B. Briggs, J. Burgess, P. M. Cullis and G. Eaton, J. Chem. Soc. Faraday Trans., 87 (1991) 1169, 88 (1992) 2871.
4 H. Matsuki, R. Ichikawa, S. Kaneshina, H. Kamaya and I. Ueda, J. Colloid Interface Sci., 181 (1996) 362.
5 M. Yoneda, K. Endoh, H. Suga and H. Hirata, Thermochim. Acta, 289 (1996) 1.
6 B. Cabane, J. Phys. Chem., 81 (1977) 1639.
7 J. François, J. Dayantis and J. Sabbadin, Eur. Polym. J., 46 (1985) 165.
8 R. Zana, J. Lang and P. Lianos, Microdomains in Polymer Solutions, Dubin P. Ed., Plenum, New York, (1985) 357.
9 B. Cabane and R. Duplessix, Colloids Surf., 13 (1985) 19.
10 C. Tondre, J. Phys. Chem., 89 (1985) 5101.
11 G. Wang and G. Olofsson, J. Phys. Chem., 99 (1995) 5588.
12 G. Olofsson and G. Wang, Pure Applied Chem., 66 (1994) 527.
13 H. Hoffmann, H. Rehage, W. Schorr and H. Thurn, Surfactants in Solution, K. L. Mittal and B. Lindman eds, Plenum (1982) 415.
14 C. A. Bunton and C. P. Cowell, J. Colloid Interface Sci., 122 (1988) 154.
15 T. Shikata, H. Hirata and T. Kotaka, Langmuir, 3 (1987) 1081.
16 H. Hoffman and H. Rehage, Surfactants Solutions: New Methods of Investigation, R. Zana ed., Dekker, (1987) 209.
17 J. C. Cobos, I. Garcia, C. Casanova, A. H. Roux, G. Roux-Desgranges and J.-P. E. Grolier, Fluid Phase Equil., 69 (1991) 223.
18 G. S. Kell, J. Chem. Eng. Data, 12 (1977) 66.
19 H. F. Stimson, Amer. J. Phys., 23 (1955) 614.
20 G. Roux-Desgranges, A. H. Roux and A. Viallard, J. Chim. Phys., 82 (1985) 441.
21 F. Quirion and J. E. Desnoyers, J. Colloid Interface Sci., 112 (1986) 565.
22 K. Busserolles, G. Roux-Desgranges and A. H. Roux, Thermochim. Acta, 259 (1995) 49.
23 K. Ballerat-Busserolles, G. Roux-Desgranges and A. H. Roux, Langmuir, 13 (1997) 1946.
24 H. Nakayama, K. Shinoda and E. Hutchinson, J. Phys. Chem., 70 (1966) 3502.
25 Z. Gao, R. E. Wasylishen and J. C. T. Kwak, J. Phys. Chem., 95 (1991) 462.
26 K. Veggeland and T. Austad, Colloids Surf., 76 (1993) 73.
27 K. Busserolles, G. Roux-Desgranges and A. H. Roux, Progr. Colloid Polym. Sci., 105 (1997) 326.
28 D. R. Scheuing and J. G. Weers, Colloids and Surfaces, 55 (1991) 41.